Characterization of Crystallization in Syndiotactic Polystyrene Thin Film Samples

Hew-Der Wu, I-Der Wu, and Feng-Chih Chang*

Institute of Applied Chemistry, National Chiao-Tung University, Hsin-Chu, Taiwan 30043

Introduction. Pluralistic crystallizations and how they affect polymorphic behavior of syndiotactic polystyrene (s-PS) have received considerable interest, mainly in *bulk* samples.[1−3] Also having been extensively studied is the development of α- or β-form crystals in s-PS, favored either kinetically or thermodynamically during the crystallization. Upon heating at several scanning rates, the relative fraction of α- and β-form crystals varies in *bulk* samples. This phenomenon favors the formations of α-form by heating at a high scanning rate. In contrast, the β-form crystal is a preferred means packing over α-form by heating at a low scanning rate and/or by crystallizing at higher temperatures closer to its T_m.[4−6] The above observations suggest that the crystal−crystal transformation indeed occurs when s-PS *bulk* sample contains the α-form as mentioned in previous literature.[1−6]

Our earlier study investigated the crystallization mechanism of s-PS *bulk* samples using conventional absorbance FTIR spectroscopy in our previous report.[7] FTIR was performed to distinguish the crystal form and crystallinity of s-PS. This work elucidates the effect of s-PS sample thickness on crystallization behavior in melt-, cold-, and heat-scanning crystallizations using FTIR spectroscopy.

Experimental Section. The syndiotactic polystyrene (s-PS) was kindly donated by the Industrial Technology Research Institute (HsinChu, Taiwan) and was used without further purification. The stereoregularity of the syndiotactic polystyrene consists of [rr] = 99% and is identified by the solution ^{13}C NMR spectrum.[8] The s-PS thin film samples were prepared by solution casting on a KBr disk, and its thickness was controlled to less than 10 μm, followed by covering with another KBr. The s-PS *bulk* sample was also obtained from solution casting on KBr disk with a thickness more than 100 μm. Isothermal cold- and melt-crystallization of various time intervals were performed on samples in an environmental chamber with a temperature programmable controller within an accuracy of ±0.1 °C. Next, the s-PS samples were pretreated at 320 °C for 20 min to eliminate the residual crystal memory in the melt-crystallization and then quenched by liquid nitrogen to obtain the amorphous (crystal-free) s-PS as the starting material. For cold-crystallization, the quenched s-PS sample was placed directly into the chamber at 264 °C. For the melt-crystallization, the s-PS sample was heated to 320 °C and quickly cooled (−100 °C/min) to 264 °C. All samples were prepared under a continuous nitrogen flow to minimize sample oxidation or degradation.

The crystal form and crystallinity of the s-PS were characterized by infrared spectroscopy (Nicolet AVA-

* To whom all correspondence should be addressed. E-mail: changfc@cc.nctu.edu.tw.

TAR 320 FTIR spectrometer, U.S.A.) with a resolution of 1.0 cm^{-1} at 30 °C, ranging from 940 to 820 cm^{-1}. The frequency scale was internally calibrated using a He−Ne laser, and 32 scans were single-averaged to reduce the noise. The absolute crystallinity of α- and β-forms of s-PS can be calculated from the following equations:[7]

$$C_\alpha = \frac{A_{851}/a_\alpha}{A_{841} + A_{851}/a_\alpha + A_{858}/a_\beta} \times 100\% \qquad (1)$$

$$C_\beta = \frac{A_{858}/a_\beta}{A_{841} + A_{851}/a_\alpha + A_{858}/a_\beta} \times 100\% \qquad (2)$$

where C_α and C_β represent the crystallinities of α and β-forms, respectively, A_{841}, A_{851}, and A_{858} are the area fractions of amorphous, α-, and β-form, as obtained by the absorbance areas ranging from 865 to 820 cm^{-1}. The conversion coefficients a_α and a_β (0.178 and 0.272 obtained from a previous investigation[7]) are the ratios of absorptive coefficients of A_{851}/A_{841} and A_{858}/A_{841} for α- and β-form crystal absorbances, respectively.

Results and Discussion. Table 1 summarizes the specific absorbance of s-PS in the IR spectrum ranging from 940 to 820 cm^{-1}.[9,10] The specific peaks of amorphous phase appear at 905 and 841 cm^{-1}. The specific peaks of α-form are at 901 cm^{-1} (shifted from 905 cm^{-1}) and 851 cm^{-1} (shifted from 841 cm^{-1}),[7] while the specific peaks of β-form are at 911 cm^{-1} (shifted from 905 cm^{-1}) and 858 cm^{-1} (shifted from 841 cm^{-1}).

Figure 1a shows the IR spectrum of the *bulk* s-PS sample isothermal at 320 °C for 20 min and then cooled to 30 °C at a rate of −10 °C/min. The peaks corresponding to the amorphous phase and α- and β-form crystal are apparent, implying that s-PS crystallizes to α- and β-form crystals during the cooling process. This finding corresponds to the well-known DSC trace results where two endothermic peaks corresponding to α- and β-form crystals always appear simultaneously in a normal cooling rate from the melt.[3,11−13] Parts b and c of Figure 1 show the IR spectra of the s-PS in *bulk* and in thin films which have been heated to 264 °C from 30 °C with a scanning rate of 10 °C/min and then quenched by liquid nitrogen, respectively. Both α-form peaks (901 and 851 cm^{-1}) and β-form peaks (911 and 858 cm^{-1}) appear in FTIR spectra of *bulk* samples as shown in Figure 1b. The mechanism of crystal growth has been described as follows:[11] The α-form nuclei formed at lower temperatures (less than ∼240 °C) induce the growth of α-form crystal during heating scanning. In addition to the heating scan, the α-form crystal converts into the thermodynamically favored β-form crystal at higher temperatures (greater than ∼240 °C) in s-PS *bulk* samples. Therefore, it leads to that s-PS crystallizes into α- and β-form crystals during heating to 264 °C in the *bulk* samples.

In contrast, only α-form peaks at 901 and 851 cm^{-1} appear after heating scanning up to 264 °C in thin film s-PS samples as shown in Figure 1c. This finding suggests that α-form crystals transforming to β-form crystals may be physically retarded at a high temperature (above ∼240 °C) in s-PS thin films with thickness less than 10 μm. Therefore, the s-PS thin film sample does not provide a favorable condition to overcome the energy barrier in order to induce the crystal transfor-

Table 1. Specific Characterized Absorbances of s-PS in IR Spectra Ranging from 940 to 820 cm^{-1}

morphology	position of absorbance (cm^{-1})[a]
amorphous phase	905 (s), 841 (m)
α-form crystal	901 (s), 851 (w)
β-form crystal	911 (s), 858 (w)

[a] Note: "s", "m", and "w" represent the "strong", "middle", and "weak" absorbnces in the IR spectrum, respectively.
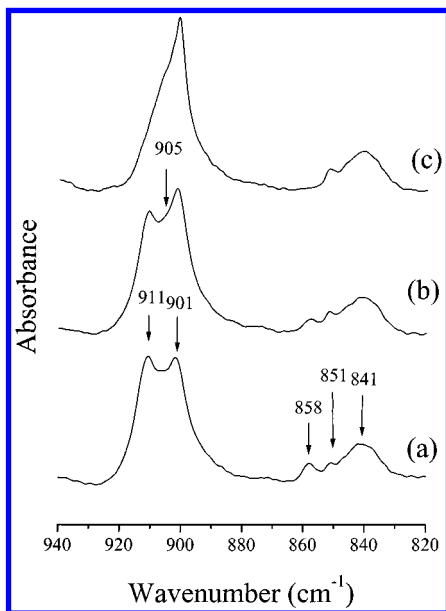

Figure 1. IR spectra of s-PS (a) *bulk* sample, cooling from 320 to 30 °C with rate of −10 °C/min; (b) *bulk* sample, heated the quenched sample to 264 °C from 30 °C with a scanning rate of 10 °C/min; and (c) thin film sample, heated the quenched sample to 264 °C from 30 °C with a scanning rate of 10 °C/min.

mation from α-form to a thermodynamically favored β-form. A critical film thickness must be met to make the α−β transformation feasible at a high temperature.

Figure 2 shows the FTIR spectra ranging from 940 to 820 cm^{-1} of the thin film s-PS sample which is melt-crystallized at 264 °C at various isothermal time durations. Notably, only two main peaks located at 905 and 841 cm^{-1} corresponding to the amorphous phase appear in Figure 2a−d where the crystallization process has not begun. The β-form characteristic peaks, 911 and 858 cm^{-1}, begin to emerge when the s-PS thin film sample is melt-crystallized at 264 °C for 20 min. Apparently, the intensity of β-form peaks gradually increases with an increasing crystallization time. Meanwhile, the relative intensity of amorphous phase peaks gradually decrease. The specific α-form peak of ∼901 cm^{-1} seems to be observed when the s-PS thin film sample is melt-crystallized at 264 °C for more than 40 min. However, the specific α-form peak of ∼851 cm^{-1} is not decomposed out after curve fitting. It is noted that the α-form may appear, but it is too weak to be apparent in the spectra. This feature corresponds to numerous earlier studies on the s-PS crystallization mechanism which shows that crystallization favors the β-form crystal at a higher temperature (i.e., above 240 °C) for thermodynamic reasons.[3]

Figure 3 shows the FTIR spectra ranging from 940 to 820 cm^{-1} of the s-PS thin film sample which is cold-crystallized at 264 °C for various isothermal time durations. The peak's intensity at 901 and 851 cm^{-1} reveals that the α-form crystal increases with an
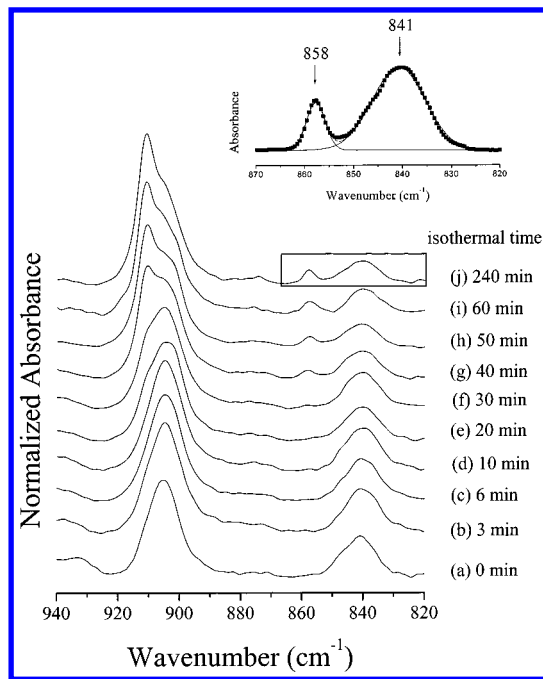

Figure 2. IR spectra of melt-crystallized s-PS thin film at 264 °C for (a) 0, (b) 3, (c) 6, (d) 10, (e) 20, (f) 30, (g) 40, (h) 50, (i) 60, and (j) 240 min durations ranging from 940 to 820 cm^{-1}. Upper-right corner shows the curve fitting ranging between 865 and 820 cm^{-1} for (j).
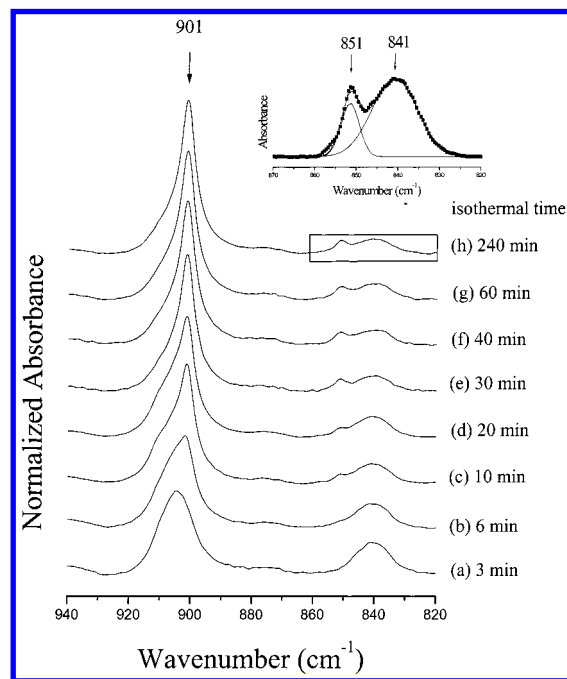

Figure 3. IR spectra of the cold-crystallized s-PS thin film at 264 °C for (a) 3, (b) 6, (c) 10, (d) 20, (e) 30, (f) 40, (g) 60, and (h) 240 min durations ranging from 940 to 820 cm^{-1}. Upper-right corner shows the curve fitting ranging between 865 and 820 cm^{-1} for (h).

increasing crystallization time; meanwhile, the relative intensity of the amorphous phase at 905 and 841 cm^{-1} decreases. From this observation, we can infer that the original α-form crystal becomes more perfect with an increasing crystallization time at 264 °C, which is reflected by the sharpening of 901 and 851 cm^{-1} peaks. However, this crystal does not convert into the thermodynamically favored β-form crystal as well as the *bulk* sample does in the cold-crystallization process. In other

Table 2. Results of Curve Fitting Ranging between 865 and 820 cm^{-1}, Absolute Crystallinity of Melt-Crystallized, and Cold-Crystallized s-PS at 264 °C for 240 min; Results from Figure 2j and Figure 3h

isothermal time of 240 min	amorphous phase			crystal phase			absolute crystallinity
	area	freq,^{a} cm^{-1}	width^b	area	freq,^{a} cm^{-1}	width^b	
cold-crystallization	0.410	840.81	10.836	0.113	851.49	4.370	60.8 (C$_\alpha$, %)^c
melt-crystallization	0.366	840.85	10.699	0.076	857.76	3.848	43.2 (C$_\beta$, %)^d

^{a} Wavenumber. ^{b} Width at half-height, cm^{-1}. ^{c} Absorptivity ratio of $A_{851}/A_{841} = 0.178$. ^{d} Absorptivity ratio of $A_{858}/A_{841} = 0.272$.

words, the individual lamellae of α-form crystals can extend upon annealing at 264 °C in s-PS thin film samples.

Comparing Figure 2 and Figure 3 reveals that the intensity of α-form peaks grows more rapidly than the corresponding β-form. Results obtained from curve fitting ranging between 865 and 820 cm^{-1} exhibit two main Gaussian peaks that provide an adequate fit with standard deviation square less than 10^{-8} for systems of melt- and cold-crystallization at 264 °C for 240 min, as shown in the upper-right corners of Figure 2 and Figure 3, respectively. Table 2 summarizes the curve-fitting results of Figure 2j and Figure 3h. The absolute crystallinity of the β-form is 43.2% in the melt-crystallization; meanwhile, that of the α-form is 60.8% in cold-crystallization, calculated from eqs 1 and 2, as the s-PS is crystallized isothermally at 264 °C for 240 min. Notably, the crystallization rate of the β-form appears to be slower than that of α-form in thin film samples.

Conclusions. In s-PS *bulk* samples, the α-form can convert into the thermodynamically favored β-form packing when the temperature is close to the T_m. In s-PS thin film samples, the α-form crystal formed at lower temperatures continues to grow along with an elevating temperature during cold-crystallization. The usually observed α- to β-form transformation at higher temperatures (above 240 °C) does not occur in thin film s-PS samples. The energy barrier of α- to β-form transformation cannot be overcome, possibly owing to the physical hindrances in very thin film samples; therefore, such a transformation of crystal form is inhibited.

Results obtained from crystallinity indicated that the crystallization of the β-form has an activation energy exceeding that of the α-form in thin film samples.

References and Notes

(1) Kellar, E. J. C.; Galiotis, C.; Andrews, E. H. *Macromolecules* **1996**, *29*, 3515.
(2) Nakaoki, T.; Kobayashi, M. *J. Mol. Struct.* **1991**, *242*, 315.
(3) Sun, Y. S.; Woo, E. M. *Macromolecules* **1999**, *32*, 7836.
(4) Woo, E. M.; Sun, Y. S.; Lee, M. L. *Polym. Commun.* **1998**, *40*, 4425.
(5) Woo, E. M.; Wu, F. S. *Macromol. Chem. Phys.* **1998**, *199*, 2041.
(6) Vittoria, V.; Ruvolo, F. A.; de Candia, F. *J. Macromol. Sci., Phys.* **1992**, *B31*, 133.
(7) Wu, H. D.; Wu, S. C.; Chang, F. C. *Polymer*, in press.
(8) Wang, Y.; Herron, N. *J. Phys. Chem.* **1991**, *95*, 525.
(9) Musto, P.; Tavone, S.; Guerra, G.; De Rosa, C.; *J. Polym. Sci., Part B: Polym. Phys.* **1997**, *35*, 1055.
(10) Wu, H. D.; Tseng, C. R.; Chang, F. C. *Macromolecules*, in press.
(11) Arnauts, J.; Berghmans, H. *Polym. Commun.* **1990**, *31*, 343.
(12) Guerra, G.; Vitagliano, V. M.; De Rosa, C.; Petraccone, V.; Corradini, P. *Macromolecules* **1990**, *23*, 1539.
(13) Sun, Z.; Morgan, R. J.; Lewis, D. N. *Polymer* **1992**, *33*, 660.

MA9919763